Differential acceptance of the COSY-11 detection system

C. Piskor-Ignatowicz* and J. Smyrski* for the COSY–11 collaboration

The COSY-11 detection system allows for measurements of meson production cross sections in the proton-proton collisions almost with a 4π acceptance close to threshold. At higher energies the acceptance drops rapidly and e.g. for the $pp \to pp\eta$ reaction at the excess energy $Q = 40$ MeV it is equal to 0.6% only. On the other hand, measurements at higher energies, where the interference effects between partial waves start to play an important role, deliver additional information about the reaction mechanism. In order to check for a possibility of measuring angular distributions at higher energies we performed studies of the influence of the limited COSY-11 acceptance on the measured differential cross sections. For this we performed simulation of the $pp \to pp\eta$ measurements at $Q = 15.5$ MeV and 40 MeV using the COSY-11 simulation package based on the GEANT-3 code. For each energy 10^7 events was generated under assumption of a uniform phase space distribution of the final states. Asymmetries of the angular distributions were introduced by multiplication the weights of events w^l by factors f^1 or f^2 corresponding to the $Ss-Sd$ and $Ss-Ds$ interference term in the expression for the $pp \to pp\eta$ differential cross section given in Ref.[1]:

$$f^1 = p_\eta^2 F_{SS}(q) cos^2\theta_\eta,$$
$$f^2 = q^2 F_{SD}(q) cos^2\theta_{pp}, \quad (1)$$

where p_η is the η momentum, $2q$ is the relative momentum of the final protons, θ_η and θ_{pp} are the angles that the η momentum and the $p-p$ relative momentum make with respect to the beam direction, F_{SS} and F_{SD} are enhancement factors accounting for the proton-proton FSI. According to Eq. 1 the factors f^1 and f^1 introduce asymmetries in the $cos\theta_\eta$ and $cos\theta_{pp}$ distributions, respectively. For histograming purposes we performed binning over $cos\theta_\eta$, $cos\theta_{pp}$ and p_η with bins numerated by indices i, j and k, respectively. Angular distributions of the cross sections were calculated according formulas:

$$\sigma_T^{1(2)}(\theta_\eta^i) = \frac{d\sigma^{1(2)}}{dcos\theta_\eta}(\theta_\eta^i) = \sum_{j,k}\sum_{l\in gen} w_{ijk}^l f_{ijk}^{1(2)}, \quad (2)$$

$$\sigma_T^{1(2)}(\theta_{pp}^j) = \frac{d\sigma^{1(2)}}{dcos\theta_{pp}}(\theta_{pp}^j) = \sum_{i,k}\sum_{l\in gen} w_{ijk}^l f_{ijk}^{1(2)}, \quad (3)$$

where the summation $\sum_{l\in gen}$ runs over all generated events and the superscripts 1 and 2 refer to inclusion of the factor f^1 and f^2, respectively. As one can expect, while the $\sigma_T^1(\theta_\eta)$ and $\sigma_T^2(\theta_{pp})$ cross sections are asymmetric (see solid line in Figs. 1a, 2b, 3a, 4b), the $\sigma_T^2(\theta_\eta)$ and $\sigma_T^1(\theta_{pp})$ distributions are completely flat (see solid line in Figs. 1b, 2a, 3b, 4a). Further on we refer to these cross sections as theoretical ones.

Cross sections reconstructed on the basis of events lying within the COSY-11 acceptance were determined as:

$$\sigma^{1(2)}(\theta_\eta^i) = \frac{d\sigma^{1(2)}}{dcos\theta_\eta}(\theta_\eta^i) = \sum_{j,k}\frac{1}{A_{ijk}}\sum_{l\in acc} w_{ijk}^l f_{ijk}^{1(2)}, \quad (4)$$

$$\sigma^{1(2)}(\theta_{pp}^j) = \frac{d\sigma^{1(2)}}{dcos\theta_{pp}}(\theta_{pp}^j) = \sum_{i,k}\frac{1}{A_{ijk}}\sum_{l\in acc} w_{ijk}^l f_{ijk}^{1(2)}, \quad (5)$$

where summation $\sum_{l\in acc}$ runs over the accepted events and A_{ijk} is an acceptance calculated as:

$$A_{ijk} = \sum_{l\in acc} w_{ijk}^l \;/\; \sum_{l\in gen} w_{ijk}^l. \quad (6)$$

One can check it easily that under assumption of $A_{ijk} \neq 0$ in the whole (i,j,k) space the $\sigma^{1(2)}$ cross sections are identical with the theoretical cross sections $\sigma_T^{1(2)}$. Indeed, at $Q = 15.5$ MeV, the $\sigma^{1(2)}$ cross sections, represented in Figs. 1, 2 by dashed-dotted line, overlap or lie very close to the $\sigma_T^{1(2)}$ cross sections. However, at $Q = 40$ MeV these cross sections (dashed-dotted line in Figs. 3, 4) lie far below the $\sigma_T^{1(2)}$ cross sections. This is caused by the fact that at higher energies the A_{ijk} acceptance is equal to zero in a large part of the (i,j,k) space. In order to avoid problems with zero values of the acceptance we introduced a kind of integrated acceptance defined as:

$$A_{ik} = \sum_j \sum_{l\in acc} w_{ijk}^l \;/\; \sum_j \sum_{l\in gen} w_{ijk}^l. \quad (7)$$

This acceptance is used for calculation of $\sigma^{1(2)}(\theta_\eta)$ and is different from zero for all allowed values of p_η and $cos\theta_\eta$ as shown in the upper part of Fig. 5. For determination of $\sigma^{1(2)}(\theta_{pp})$ analogically defined acceptance A_{jk} is used. It has "a hole" for small values of p_η and $cos\theta_{pp}$ (see lower part of Fig. 5). The cross sections calculated with the use of these acceptances are represented by dashed lines in Figs. 1-4. They reproduce the theoretical cross sections in the case of the asymmetrical distributions quite well but deviate seriously from the flat distributions.
We did also calculations with acceptance summed additionally over the index k

$$A_i = \sum_{j,k} \sum_{l\in acc} w_{ijk}^l \;/\; \sum_{j,k} \sum_{l\in gen} w_{ijk}^l. \quad (8)$$

This acceptance was applied in Eq. 4 and for Eq. 5 an analogically calculated acceptance A_j was used. Results are represented by dotted lines in Figs. 1-4. The deviations from the theoretical cross sections are relatively large – of the order of seventy percent.

In conclusion we want to state that the acceptance A_{ijk} calculated as a function in the three dimensional space (i,j,k) allows for a very good reproduction of angular

distributions at $Q = 15.5$ MeV. It fails, however, at $Q = 40$ MeV due to dominance of zero values of A_{ijk}. The integrated acceptances A_{ik} and A_i do not lead to satisfactory results neither at $Q = 15.5$ MeV nor at $Q = 40$ MeV.

* Institute of Physics, Jagellonian University, 30–059 Cracow, Poland

References:

[1] H. Calén et al., Phys. Lett. B 458 (1999) 190

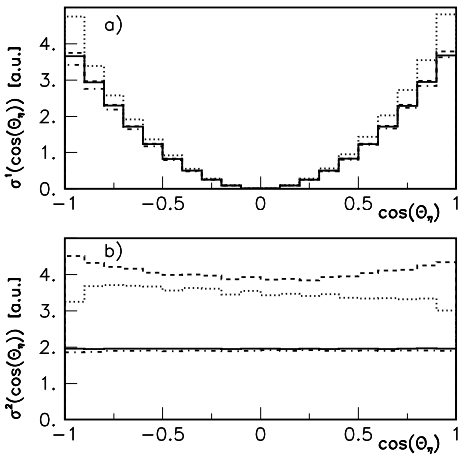

Figure 1: $\sigma^{1(2)}(\theta_\eta)$ at $Q = 15.5$ MeV

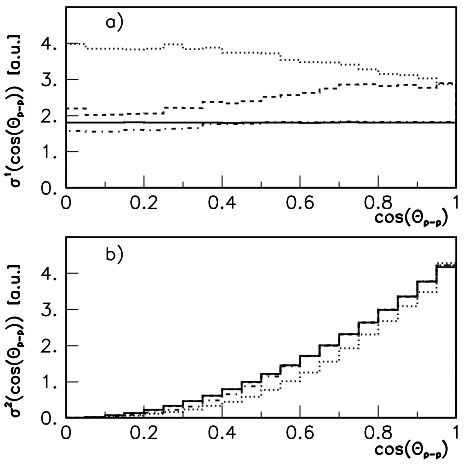

Figure 2: $\sigma^{1(2)}(\theta_{pp})$ at $Q = 15.5$ MeV

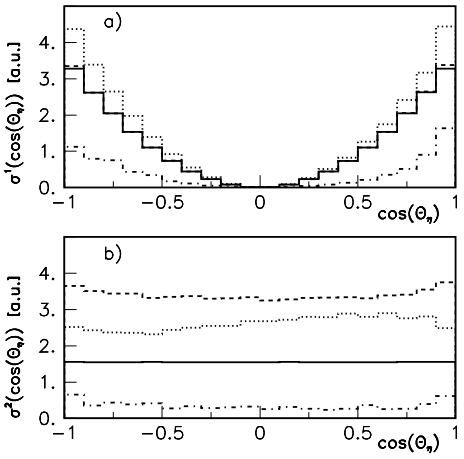

Figure 3: $\sigma^{1(2)}(\theta_\eta)$ at $Q = 40$ MeV

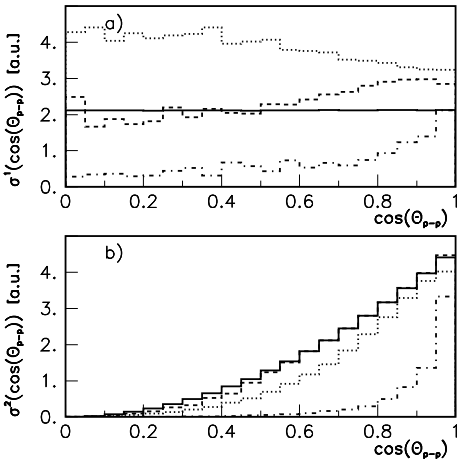

Figure 4: $\sigma^{1(2)}(\theta_{pp})$ at $Q = 40$ MeV

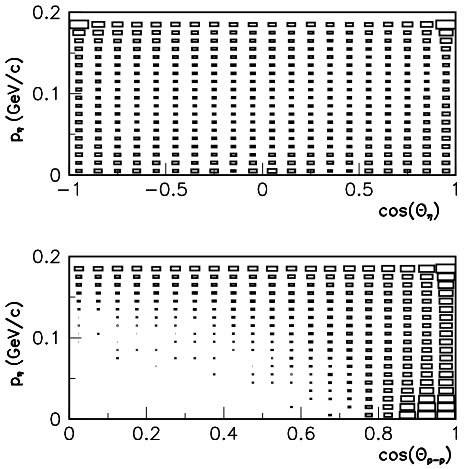

Figure 5: Acceptances A_{ik} and A_{jk} at Q=40 MeV.